



Improvement of phase map quality for Michelson interferometer based spatial phase-shift digital shearography

Xin Xie¹, Junrui Li¹, Bin Zhang^{1,4}, Liping Yan^{1,3}, and Lianxiang Yang^{1,2}

¹Optical Laboratory, Department of Mechanical Engineering, Oakland University, Rochester, Michigan, 48309, USA

²School of Instrument Science and Opto-electronics Engineering,
Beijing Information Science and Technology Beijing, 100192, China

³Nanometer Measurement Laboratory, Zhejiang Sci-Tech University, Hangzhou, 310018, China

⁴Department of Physics, Beijing Jiaotong University, Beijing, 100044, China

Dedicated to Padmashree Prof R S Sirohi, FNAE

The recently fast developed spatial phase-shift digital shearography technique suits well for non-destructive testing and strain measurement under continuous/dynamic loading condition which greatly extended the application range of digital shearography. However, the phase map quality of the spatial phase shift digital shearography is usually relatively low comparing to conventional temporal phase-shift based digital shearography. This paper introduces a series of new developments on improving the phase map quality for Michelson Interferometer based spatial phase-shift digital shearography including using innovated optical path design, aperture design and directional enhanced smoothing algorithm. The theory, optical analysis, experimental setup and data comparison are shown in detail in this article.

© Anita Publications. All rights reserved.

Keywords: Digital shearography, Michelson Interferometer, Temporal phase-shift

1 Introduction

Digital Shearography (DS) is a non-contact, whole field, high sensitivity optical measurement method which has the capability of measuring strain information directly. With the introduction of phase-shift technique, the measurement sensitivity of digital shearography has been increased by tens of times comparing to the fringe counting based technology [1]. The phase-shift digital shearography can be divided into two categories according to their phase-shift method: the temporal phase-shift digital shearography (TPS-DS) and the spatial phase-shift digital shearography (SPS-DS). The temporal phase-shift technique solves the phase information by introducing multiple phase stepping steps along time history. However, it requires the speckle pattern distribution keeps stable during the multiple phase stepping steps which limits its application to a static loading or step-by-step loading situation only. The spatial phase-shift digital shearography solves the phase information by introducing additional spatial frequencies which does not require multiple phase stepping steps along time history, thus enabled the phase evaluation using single speckle pattern image. This significant advantage makes it an ideal tool for the measurement under continuous/dynamic loading condition [2, 3].

The first spatial phase-shift digital shearography system is reported by G Pedriniet al in 1996 [4]. In this setup, a Mach-Zehnder interferometer was used to form two sheared images and create the carrier frequency. However, due to the high complexity and low light efficiency of the setup, the phase map quality was poor and also the measurement area was very small. Bhaduri et al introduced another type of spatial phase-shift digital shearography by using a multiple-aperture mask in 2006 [5,6]. The multi-aperture based spatial-phase shift digital shearography provides a much better phase map quality, however, due to the use of collimate illumination, the measurement area was greatly limited. In 2013, Xie et al introduced a 4f system embedded Michelson Interferometer based spatial phase-shift digital shearography system. The Michelson Interferometer provides a high light efficient and simple structure which provides relatively better phase map quality compared to G Pedrini's system. Also by working with a 4f system, it also provides an adjustable

Corresponding author :

e-mail: yang2@oakland.edu; Fax : (+1)248-370-4416 (Lianxiang Yang)

measurement area (from 1mm^2 to 1m^2) [7-9]. However, due to a low utilization rate of the spectrum, the phase map quality was still not comparable to the phase maps created by temporal phase-shift method.

This article shows that, by introducing the slit aperture and directional enhanced smoothing algorithm, the phase map quality of the Michelson Interferometer based SPS-DS can be greatly improved. Basic theory, speckle pattern and spectrum analysis and a group of comparison experiments are shown in detail.

2 Methodology and Comparison

Figure 1 shows the schematic of a 4f system embedded Michelson Interferometer based spatial phase-shift digital shearography setup. A beam expander (BE) expands an Optically Pumped Semiconductor Lasers (OPSL) laser (Coherent Verdi G5), with a wavelength of 532nm , to illuminate the testing object. The diffused light reflected from the object goes through the shearing device and is imaged on the CCD plane. In this setup, a Michelson Interferometer is used as the shearing device. One mirror of the Michelson Interferometer (M1) is tilted to form a small shearing angle. This shearing angle introduces a shearing amount on the speckle pattern image to form a shearogram and also introduces a carrier frequency which can be used to separate spectra on the frequency domain. A 4f system, which consists of two lenses (L1 and L2), is embedded to enlarge the field of view. Both lenses have a focal length of 100mm . The shearogram is recorded by a high resolution CCD camera (2456×2058 pixels, with a pixel size of $(3.45 \times 3.45)\mu\text{m}$). Through the Fourier Transform, the speckle pattern image is transferred into a spectrum on the Fourier domain. The spectrums are also separated when a spatial frequency shift is introduced by the shearing. To limit the spectra size, an aperture is located at the front focal point of the image lens. The phase differences can then be calculated from the complex amplitude by applying a properly selected Windowed Inverse Fourier Transform (WIFT). By analyzing the phase difference of the laser before and after loading, the out-of-plane deformation gradient of the testing object due to the loading can be evaluated.

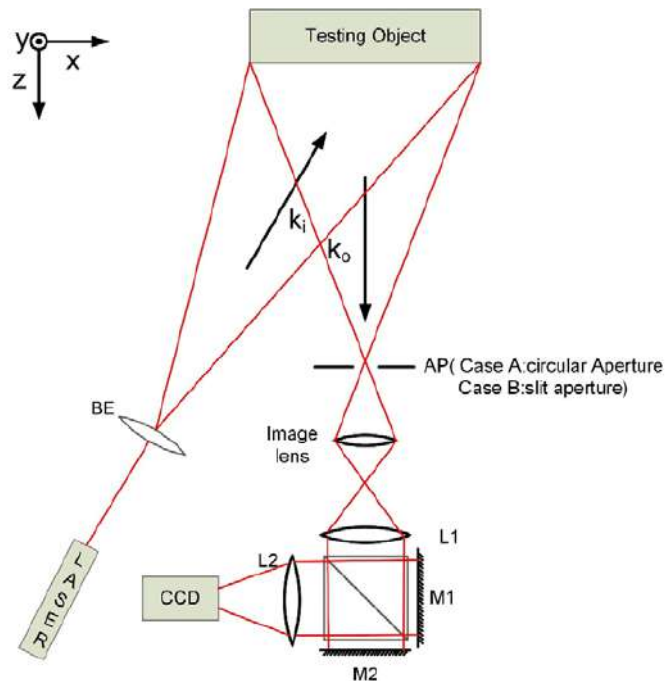


Fig. 1. Schematic of Michelson Interferometer based spatial phase-shift digital shearography

In this experiment, an edge-clamped and center loaded round metal plate is tested using this shearography system. The testing plate is loaded by a micrometer pushing the center of the plate from the back side. In order to understand the influence of the aperture shape, two cases are studied. In case A, a circular shaped aperture is used in the setup shown in Fig 1 to measure the deformation gradient of the metal plate. In case B, a slit shaped aperture is used in the setup shown in Fig 1 to measure the same deformation gradient of the metal plate.

In both cases, the CCD camera captures two shared wave fronts from the reference object and testing object. In the experiment, the shearing direction is in the x-direction. These two wave fronts can be represented by the following equations:

$$u_1(x, y) = |u_1(x, y)| \exp[i\phi(x, y)] \tag{1a}$$

$$u_2(x, y) = |u_2(x + \Delta x, y + \Delta y)| \exp\{i\phi(x + \Delta x, y + \Delta y) - 2\pi if_0 \cdot x\} \tag{1b}$$

where u_1 and u_2 are the two components of the reference object and testing object. Δx and Δy are the shearing distance in the x and y directions, respectively.

The value f_0 , which represents the component of the spatial frequency introduced by shearing angle, can be expressed as:

$$f_0 = (\sin \theta / \lambda) \tag{1c}$$

where λ is the laser wavelength and θ represents the shearing angle of the two mirrors (M1 and M2).

The intensity recorded on the CCD camera can be expressed as:

$$I = (u_1 + u_2)(u_1^* + u_2^*) = u_1u_1^* + u_2u_2^* + u_1u_2^* + u_2u_1^* \tag{2}$$

The * denotes the complex conjugate of u_i . The Fourier Transform converts the image from the spatial domain to the Fourier domain.

Figure 2 (a) and (b) show the recorded speckle pattern intensity images under 400mW illumination. Figure 2 (a) shows the speckle pattern image under a 1mm diameter circular aperture. Figure 2(b) shows the speckle pattern image under a 1mm(H) × 13.6mm(V) size slit aperture. As the slit aperture has a bigger size in vertical direction, the intensity received on CCD camera in case B is stronger, which makes Fig 2(b) brighter than Fig 2(a).

Two enlarged figures are used to show the details of the speckle pattern in and out of overlapped area for each cases. From the enlarged image (lower images) in Fig 2(a), it can be found that the speckle shape is a circular shape due to the use of circular aperture. Also, from the upper enlarged image in Fig 2(a), the carrier fringes (vertical fringes created from x directional shearing) can be clearly seen among the circular shaped speckle pattern. From the lower enlarged image in Fig 2(b), it can be found that with the use of slit aperture, the speckle pattern becomes a linear shape. This is caused by the difference of aperture size between horizontal direction and vertical direction. The speckle pattern size received on CCD camera is decided by Eq (3):

$$\Delta s = \frac{\lambda f}{D} \tag{3}$$

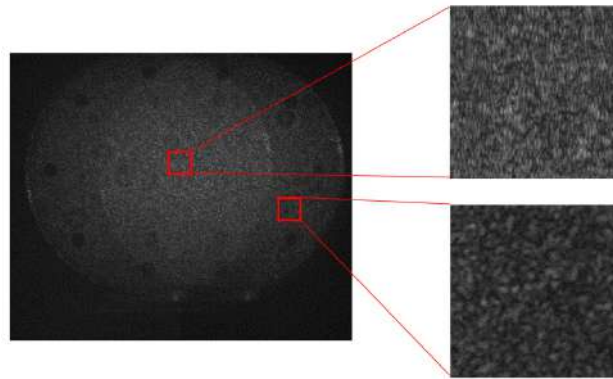
For the slit aperture, as the aperture size in horizontal direction is much smaller than the size in vertical direction, the speckle pattern size in horizontal direction becomes much bigger than the size in vertical direction making the speckle patterns a linear shape looking like shot solid lines. From the upper enlarged image in Fig 2(b), the carrier fringes (vertical fringes) can also be found. However, as the speckle

shape is linear in this situation, the vertical carrier fringes now make the speckle patterns look like dot lines.

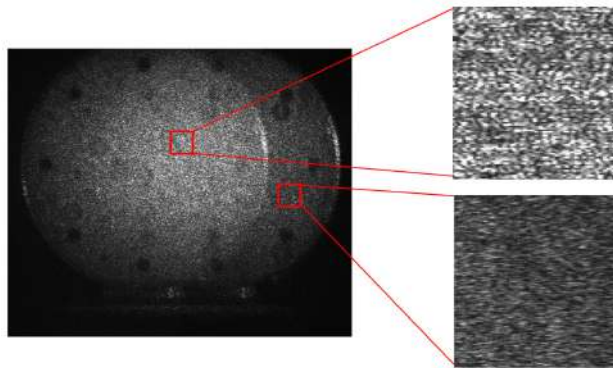
After a Fourier Transform, Eq (2) becomes:

$$\begin{aligned} \text{FT}(\mathbf{I}) = & U_1(f_x, f_y) \otimes U_1^*(f_x, f_y) + U_2(f_x + f_0, f_y) \otimes U_2^*(f_x + f_0, f_y) \\ & + U_1(f_x, f_y) \otimes U_2^*(f_x + f_0, f_y) + U_2(f_x + f_0, f_y) \otimes U_1^*(f_x, f_y) \end{aligned} \quad (4)$$

Here \otimes is the convolution operation, $U_1(f_x, f_y) = \text{FT}(u_1)$, $U_2(f_x + f_0, f_y) = \text{FT}(u_2)$.



(a)



(b)

Fig 2. Speckle pattern images under different aperture shape cases: (a) speckle pattern image under a 1mm diameter circular aperture; (b) speckle pattern image under 1mm width slit aperture.

Figures 3(a) and (b) show the Fourier spectrum of the images using a circular aperture and a slit aperture, respectively. For both cases, there are three spectra on the Fourier domain, which correspond to the four terms in Eq (4). Due to the use of different shaped apertures, the shape of the center and side spectra varies correspondingly. From the comparison of Fig 3(a) and 3(b), it can be found that under the same shearing amount and aperture size, the slit aperture provides much bigger side spectrum area which can be used to extract the phase information.

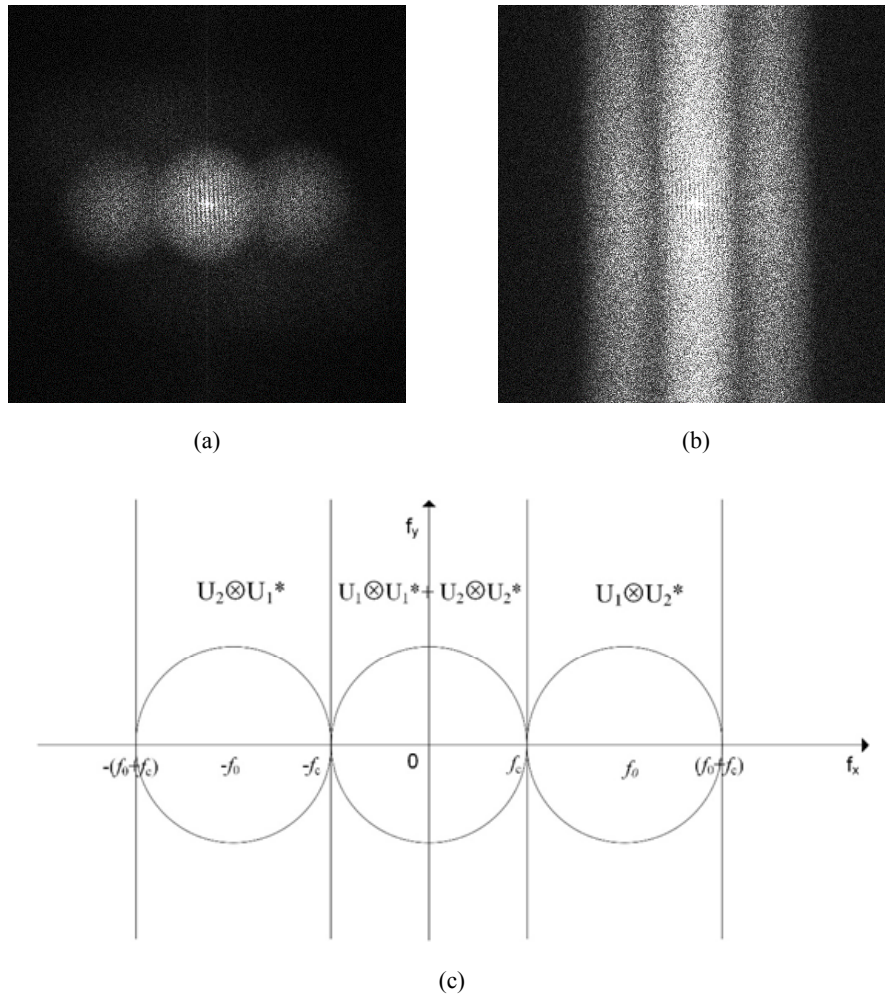


Fig 3. (a) Spectrum of speckle pattern image using a circular aperture setup; (b) Spectrum of speckle pattern image using a circular aperture setup; (c) schematic of the ideal spectrum

The four spectra are separated into three parts due to different spatial frequencies. The $U_1 \otimes U_1^* + U_2 \otimes U_2^*$ terms, which are low frequency terms mainly from the background light, are located at the center of the frequency domain. The $U_2 \otimes U_1^*$ term is located at $(-f_0, 0)$, and the $U_1 \otimes U_2^*$ term is located at $(f_0, 0)$. Both terms contain the phase information of the recorded shearogram. In order to avoid frequency aliasing, these two side spectra must be separated from the center spectra. To properly separate them, the aperture size and the shearing amount must be carefully controlled. As shown in Fig 3(c), in an ideal spectrum, in order to separate the side spectra with center spectra, the carrier frequency f_0 and the cut off frequency introduced by the aperture must meet the relationship of:

$$f_0 \geq 2f_c \tag{5a}$$

As the carrier frequency is given by Eq (1c) and the cut off frequency f_c is given by:

$$f_c = \frac{D}{2\lambda f} \tag{5b}$$

Putting Eq (1c) and Eq (5b) into Eq (5a), we have:

$$\sin \theta \geq \frac{D}{f} \quad (5c)$$

Equation (5) shows two effects. The first, under given shearing amount, the aperture size has to be set small enough to separate the spectra. On the contrary, under given aperture size D , the shearing amount has to be big enough to separate the spectra. Also, the spectra area has to be sufficiently big, otherwise the signal/noise ratio will be very low and finally result in a noisy phase map.

By applying a Windowed Inverse Fourier Transform (WIFT) on the spectra located on $(f_0, 0)$, the phase distributions can be calculated using the complex amplitudes. This results in the following equation:

$$[\theta + 2\pi x f_0] = \arctan \frac{\text{Im}[u_2 u_1^*]}{\text{Re}[u_2 u_1^*]} \quad (6)$$

For Eq (6), Im and Re denote the imaginary and real part of the complex numbers, and θ is the phase difference between the two tilted beams.

In the same sense, after the object deforms, two additional phase distributions can be obtained by the same method using the recorded images:

$$[\theta' + 2\pi x f_0] = \arctan \frac{\text{Im}[u_2 u_1^*]}{\text{Re}[u_2 u_1^*]} \quad (7)$$

The relative phase difference due to a deformation can then be calculated as:

$$\begin{aligned} \Delta = \theta - \theta' &= \frac{2\pi \cdot \Delta x}{\lambda} \mathbf{d} \cdot \mathbf{s} \\ &= \frac{2\pi \cdot \Delta x}{\lambda} \left(\frac{\partial u}{\partial x}, \frac{\partial v}{\partial x}, \frac{\partial w}{\partial x} \right) \cdot (\sin \alpha, 0, 1 + \cos \alpha) \end{aligned} \quad (8)$$

Figure 4(a) and (b) show the phase map created from a circular aperture SPS-DS setup and the phase map created from slit aperture SPS-DS setup, respectively. Figure 4(c) and Fig 4(d) show the two times 7×7 smoothed phase map of Fig 4(a) and Fig 4(b), respectively. Comparison of Fig 4(c) and Fig 4(d) shows that setup with slit aperture provides better phase map quality. The main reason is that with the circular aperture, the speckle size is very big in all directions, and finally results in small 'cracks' in phase map (as shown in the enlarged image of Fig 4(a)). However, when using the slit aperture, a bigger speckle size is generated in the horizontal direction which finally results in a better phase map quality.

As shown in Fig 3 and Eq (5), with the circular aperture the shearing amount is usually set at very big value due to its low utilization of spectrum area. That is why in the experiment shown above the shearing amount is set at an extreme big value. However, for the slit aperture SPS-DS setup, the requirement for the shearing amount is greatly reduced. To show this capability, another experiment is processed using the same setup with a slit aperture while the shearing amount and aperture size are set at half of the previous value. Figure 5 (a) shows the recorded speckle pattern image. Figure 5 (b) shows spectrum after Fourier Transform. As can be found in Fig. 5, with a 50% decreasing on the shearing amount and aperture size, the spectra still can be perfectly separated which also gives a reasonably big enough spectrum area. Figure 5(c) shows the phase map created from the slit aperture SPS-DS setup. Comparison of Fig 4(a) with Fig 5(c) shows that with the use of slit aperture, a measurement under much smaller shearing amount can be achieved without the loss of phase map quality. And also the smaller shearing amount provides bigger overlapped area of the two sheared images and finally results in a bigger measurable area.

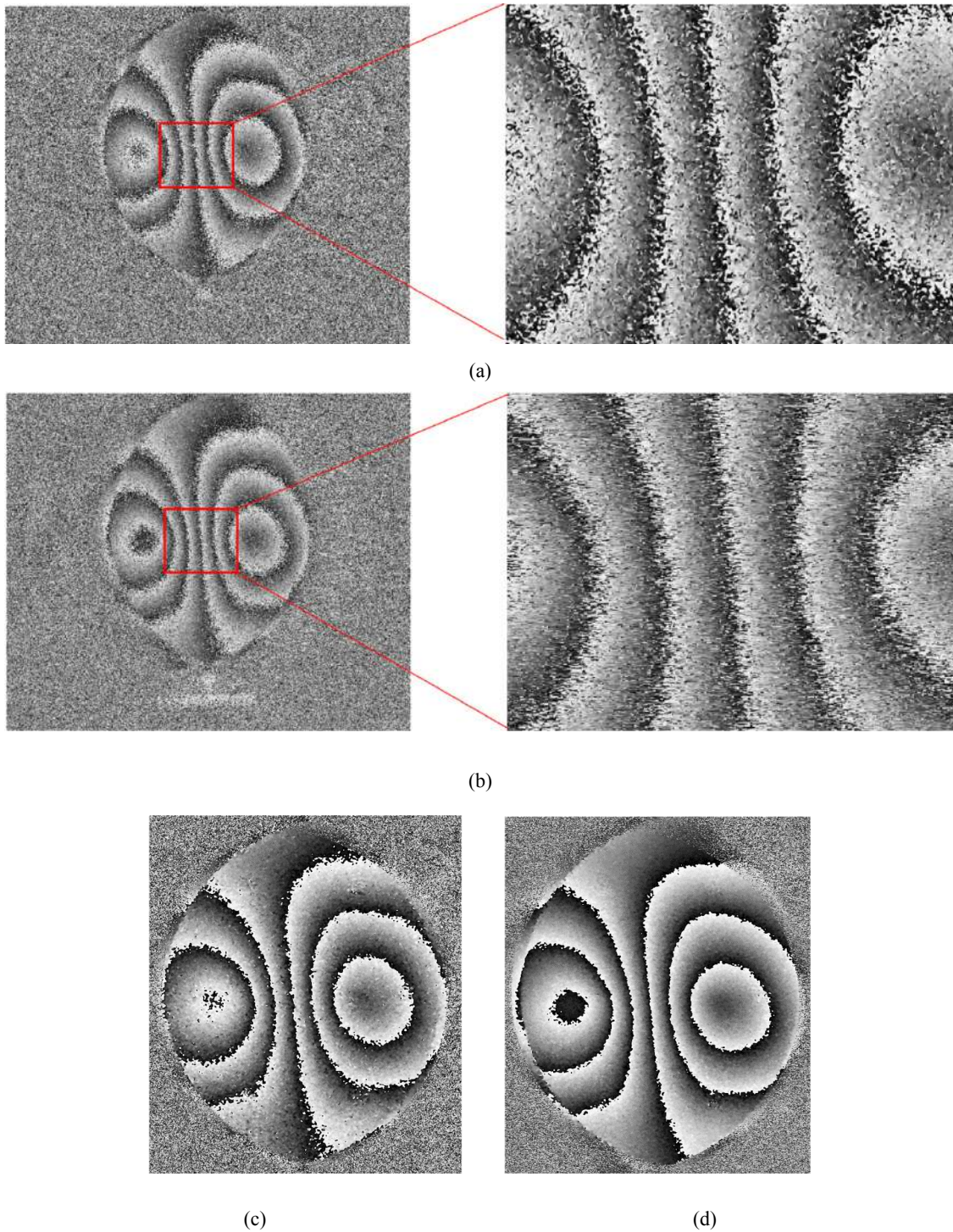


Fig 4. (a) phase map created from circular aperture ; (b) phase map created from slit aperture ; (c) 2 times 7×7 smoothed phase map created from circular aperture ; (d) 2 times 7×7 smoothed phase map created from slit aperture

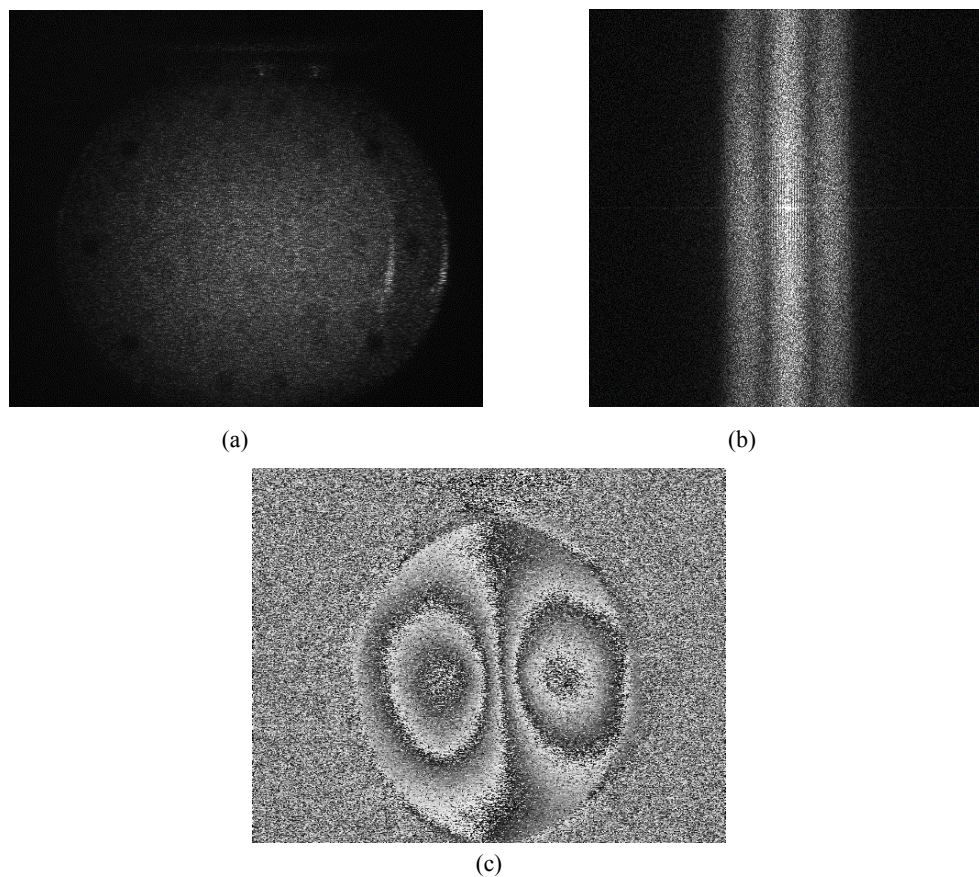
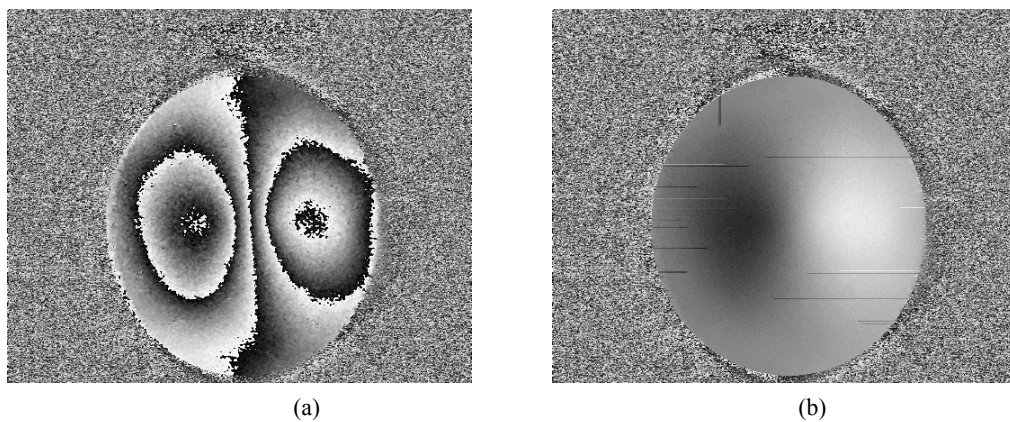


Fig 5. (a) Recorded speckle pattern image with half shearing amount; (b) spectrum of Fig 4(a); (c) extracted phase map from windowed inverse Fourier Transform of Fig 4(b).

3. Directional enhanced smoothing method

As mention above, the introduction of slit aperture provides the SPS-DS setup a higher utilization rate of spectrum, a smaller achievable shearing amount as well as a better phase map quality. However, it also brings a side effect that the speckle pattern size has a huge difference in horizontal and vertical directions.



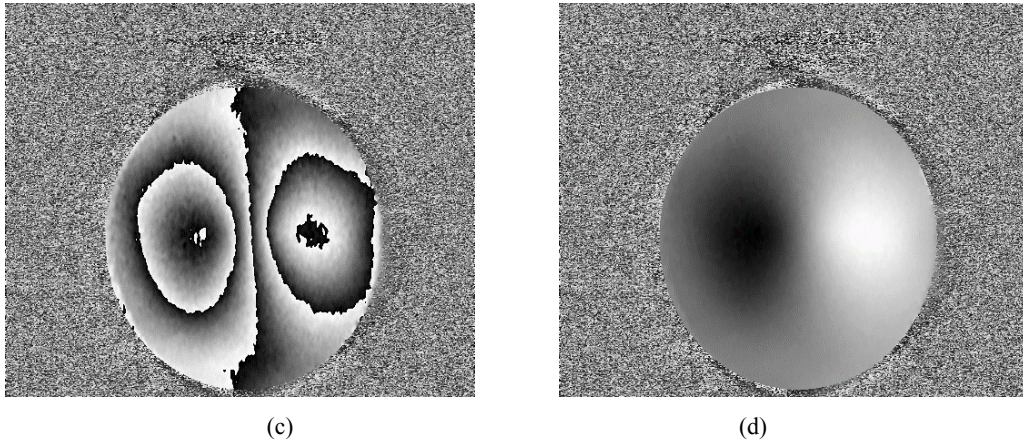


Fig 6 (a) 3 times 7×7 sin-cos smoothed phase map of Fig 5(c); (b) unwrapped phase map of Fig 6(a); (c) 3 times 715 directional enhanced sin-cos smoothed phase map of Fig 5(c); (d) unwrapped phase map of Fig 6(c).

This side effect also brings a challenge for the smoothing algorithm. Figure 6 (a) shows the smoothed phase map using a 7×7 sin-cos smooth algorithm (3 times) [10]. Figure 6(b) shows the unwrapped phase map of Fig 6(a). As shown in Fig 6(b), a lot of fail unwrapped area exists due to the high noise in Fig 6(a), especially notice that most of the noise is in horizontal direction due to the ‘horizontal lined’ speckle pattern shape [11]. In order to solve this problem, a directional enhanced 7×15 sin-cos smoothing algorithm (3 times) is latter applied to Fig 5(c). Comparing to ordinary square filtering window, a directionally enhanced filtering window has different cutoff frequency in vertical and horizontal directions. It is a fact that smaller filtering window provides lower cutoff frequency, and vice versa. Since the speckle size is bigger in horizontal direction, which means the low frequency part is stronger in horizontal direction comparing to the vertical direction. The stronger low frequency part in horizontal direction does not require a high cutoff frequency filtering window as in vertical direction. Thus lower cutoff filtering frequency should be chosen in the horizontal direction not in the vertical direction. In the used 7×15 filtering window size, it has lower cutoff frequency in the horizontal direction than in the vertical direction, which will be very suitable for our speckle size case. The directional enhanced smoothed phase map is shown in Fig 6(c). Compared with Fig 6(a), the phase map quality is significantly improved. Figure 6(d) shows the unwrapped phase map of Fig 6(c). As shown in Fig. 6(d), by using the directional enhanced smoothing algorithm, the whole phase map area can be unwrapped successfully (the horizontal fail points in Fig 6(b) have been eliminated).

4 Conclusion

This paper introduces two ways for improving the phase map quality in the Michelson Interferometer based spatial phase-shift shearography setup, by utilizing slit aperture and directional enhanced phase map filtering. A series of comparison experiments between circular aperture embedded SPS-DS and slit aperture embedded SPS-DS are processed. The results show that the slit aperture embedded SPS-DS system can provide a better phase map as well as a smaller minimum shearing amount. A comparison experiment between regular sin-cos smoothing algorithm and horizontal directional enhanced sin-cos smoothing algorithm shows that due to the linear shape of the speckle pattern in the slit aperture embedded system, the directional enhanced smoothing algorithm can be proved a much better smoothed phase map quality.

Acknowledgement

The authors wish to acknowledge the financial support of the National Natural Science Foundation of China for the funding of the project (project approval number: 51275054).

References

1. Yang Lianxiang, Frank Chen, Wolfgang Steinchen, Michael Y Hung, Digital shearography for nondestructive testing: potentials, limitations, and applications, *J Holography and Speckle*, 1(2004)69-79.
2. Xie Xin, Xiaona Li, Xu Chen, Lianxiang Yang, Review of recent developments of spatial phase-shift digital shearography, In International Conference on Experimental Mechanics, (2014) 93020E-93020E, Singapore, November 15, 2014.
3. Pedrini G, Osten W, Gusev M E, High-speed digital holographic interferometry for vibration measurement, *Appl Opt*, 45(2006)3456-3462.
4. Pedrini G, Zou Y-L, Tiziani H J, Quantitative evaluation of digital shearing interferogram using the spatial carrier method, *Pure Appl Opt*, 5(1996)313.
5. Bhaduri B, Mohan N K, Kothiyal M P, Sirohi R S, Use of spatial phase shifting technique in digital speckle pattern interferometry (DSPI) and digital shearography (DS), *Opt Express*, 14(2006)11598-11607.
6. Bhaduri B, Mohan N K, Kothiyal M P, Simultaneous measurement of out-of-plane displacement and slope using a multiaperture DSPI system and fast Fourier transform, *Appl Opt*, 46(2007)5680-5686.
7. Xie X, Yang L X, Xu N, Chen X, Michelson interferometer based spatial phase shift shearography, *Appl Opt*, 52(2013)4063-4071.
8. Xie X, Xu N, Sun J, Wang Y, Yang L X, Simultaneous measurement of deformation and the first derivative with spatial phase-shift digital shearography, *Opt Commun*. 286(2013)277-281.
9. Xie X, Zheng Y, Li X, Sia B, Zhong P, Yang G, Yang L, Spatial Phase-Shift Digital Shearography for Out-of-Plane Deformation Measurement, *SAE International Journal of Materials and Manufacturing*, 7(2014) 402-405.
10. Steinchen W, Yang L, Digital shearography: theory and application of digital speckle pattern shearing interferometry, Chapter 3, (Bellingham: SPIE Press), 2003, pp 92-99.
11. Herráez M A , Burton D R, Lalor M J, Gdeisat M A, Fast two-dimensional phase-unwrapping algorithm based on sorting by reliability following a noncontinuous path, *Appl Opt*, 41(2002)7437-7444.

[Received:16.7.2015; accepted:1.8.2015]

Dr. LIANXIANG YANG received his Ph D in Mechanical Engg from the University of Kassel, Germany in 1997. He is Professor of Mechanical Engineering in Oakland University, USA and the director of the advanced optical research group. Professor Yang's research is in the cutting edge area of advanced optical metrology, which focuses on the development and application of advanced optical methods such as digital image correlation, digital laser speckle interferometry/digital holography, and digital shearography to analyze and solve a wide ranging number of engineering problems. He has published 4 books and book chapters, 7 journal or proceeding editorials, over 180 peer reviewed papers, and applied for 11 patents. In the past 10 years, Dr. Yang also delivered several invited talks, research seminars, and keynote presentations in US and abroad. Prof. Yang is a Fellow of SPIE and was the Chair of Material Modeling and Testing Committee of SAE from 2000 to 2012. He is currently serving as an Associate Editor or on Editor Board of 5 SCI journals, such as *Optical Engineering*, *Optics and Lasers in Engineering* etc.



XIN XIE is a Ph. D. candidate working in the Optical Laboratory of Mechanical Engg at Oakland University (OU). He received his master's degree in Mechanical Engg from Oakland Univ, USA, in 2012. His research field includes optical metrology, phase-shift technology, speckle pattern interferometry, digital image correlation and nondestructive testing.



JUNRUI LI is a Ph. D student in the Optical Laboratory of Mechanical Engg at Oakland University. He received his master's degree in Instrumental Engineering from Hefei University of Technology, China, in 2014. His research field includes optical metrology, speckle pattern interferometry, digital image correlation and nondestructive testing.



Dr. Bin Zhang, obtained her BSc and MSc from Changchun Institute of Optics and Fine Mechanics in 1994 and 1997, respectively. She then completed her PhD at Changchun Institute of Optics Fine Mechanics and Physics, Chinese Academy of Sciences in 2000. She went to National Key Lab of Advanced Photonic Materials and Devices in FuDan University as a post doctor in the same year. Now, she worked in the Department of Physics, Beijing Jiaotong University. She was a visiting scholar at Oakland University from July 2014 to July 2015. The research is related to optoelectric detecting, optical system and photonic materials and devices.



Dr. LIPING YAN received her Ph D in Mechanical Manufacture and Automation from Zhejiang Sci-Tech University, Hangzhou, China in 2014. She is an Associate Professor of School of Information Science and Technology, Zhejiang Sci-Tech University, Hangzhou, China since 2011. She was a visiting scholar at Oakland University from February 2015 to October 2015. Her research interests include laser interferometer, precision measurement metrology and photoelectric signal processing.

